Human fatty acid synthase mRNA: tissue distribution, genetic mapping, and kinetics of decay after glucose deprivation[1]

Clay F. Semenkovich,[2,]* Trey Coleman,* and Fred T. Fiedorek, Jr.†

Department of Medicine and Department of Cell Biology and Physiology,* Washington University School of Medicine, St. Louis, MO 63110, and Department of Medicine,† University of North Carolina, Chapel Hill, NC 27599-4735

Abstract To better understand the accelerated decay of fatty acid synthase (FAS) message that occurs after glucose deprivation (*J. Biol. Chem.* 1993. **268:** 6961–6970), we characterized the 3′ terminus of the human message and the kinetics of FAS mRNA decay in HepG2 cells. The FAS gene was localized to human chromosome 17q24-25 and to syntenic distal mouse chromosome 11. Expression of the FAS message in human tissues was ubiquitous with high levels in liver, lung, and intra-abdominal adipose tissue. The 806 nucleotide 3′ untranslated region of the human mRNA contained two regions with the instability pentamer AUUUA. Unlike short-lived messages containing AUUUA motifs, FAS mRNA decay after glucose deprivation was not first order, and there were no detectable changes in the poly(A) tail. Glucose deprivation transiently caused FAS message to sediment more rapidly than control message in density gradients. In vivo treatment with different translational inhibitors showed that translation per se was not necessary for FAS mRNA decay; association of polysomes with FAS message protected it from decay. In cell-free decay experiments, FAS mRNA decay was more rapid using components from glucose-deprived than glucose-treated cells. These data suggest that glucose regulates cytoplasmic HepG2 FAS mRNA stability by partitioning the message between a translated pool not subject to degradation and a decay compartment, features reminiscent of regulated stability for other diet-responsive messages.—**Semenkovich, C. F., T. Coleman, and F. T. Fiedorek, Jr.** Human fatty acid synthase mRNA: tissue distribution, genetic mapping, and kinetics of decay after glucose deprivation. *J. Lipid Res.* 1995. **36:** 1507–1521.

Supplementary key words message stability · AU-rich elements · adipose tissue · mouse fatty acid synthase gene · lipogenesis

Fatty acid synthase (FAS), the multifunctional protein that synthesizes palmitate from acetyl CoA, malonyl CoA, and NADPH, is regulated by diet and may be rate limiting in the long-term production of fatty acids (1). Dietary regulation of this enzyme is predominantly mediated by changes in FAS gene transcription (2). However, other mechanisms, in particular alteration of mRNA stability, may also contribute to FAS regulation. Carbohydrate feeding appears to increase both transcription and mRNA stability for FAS in rat liver (reviewed in ref. 3), and we have recently shown that glucose regulates FAS enzyme activity in human HepG2 cells by affecting FAS message stability (4). Alteration of mRNA stability also contributes to regulation of FAS gene expression in fetal rat lung (5), human breast cancer cell lines (6), and mouse 3T3-L1 preadipocytes (7). It is not surprising that nutritional regulation of FAS expression could involve message stability; carbohydrates regulate mRNA stability for other lipogenic enzymes including glucose-6-phosphate dehydrogenase, malic enzyme, and L-pyruvate kinase (2) although for each of these enzymes, regulation is primarily transcriptional.

Little is known about the mechanisms of regulated message stability in mammalian cells. Previous studies have focused on two general features of message decay, the role of structural elements within the message, and the relationship of translation to decay. Two well-known structural elements in mammalian messages are the iron-responsive element and the AU-rich element. The iron-responsive element is a stem–loop structure in the

Abbreviations: FAS, fatty acid synthase; PEPCK, phosphoenolpyruvate carboxykinase; PCR, polymerase chain reaction; SSLP, simple sequence length polymorphism; IRE, iron-responsive element; DRB, dichloro-ribofuranosylbenzimidazole.

[1]This work was presented at the 67th Scientific Session of the American Heart Association, Dallas, TX, 1994 (*Circulation.* **90 No. 4, Part 2:** I-352).

[2]To whom correspondence should be addressed at: Division of Atherosclerosis, Nutrition and Lipid Research, Washington University School of Medicine, 660 South Euclid Avenue, Box 8046, St. Louis, MO 63110.

3′ untranslated region of the transferrin receptor message that promotes decay (8). Also located in the 3′ untranslated region are AU-rich elements, sequences characterized by the presence of one or more copies of the pentamer AUUUA in a region with high AU content. These elements are probably responsible for the intrinsic lability of cytokine and proto-oncogene messages (9) and can mediate hormone-induced regulation of message decay (10).

Ongoing translation is necessary for the decay of most short-lived messages containing AU-rich elements which may be explained by ribosome-associated nucleases (11). Savant-Bhonsale and Cleveland (12) recently provided an additional potential link between translation and AUUUA motif-associated message decay. They identified a potential degradation complex for the GM-CSF mRNA that required 3′ untranslated region AUUUA motifs and active translation.

A separate class of messages is characterized by a different interaction with ribosomes. The mRNAs for phosphoenolpyruvate carboxykinase (PEPCK, 13), tyrosine aminotransferase (14), vitellogenin (15), and vasoactive intestinal peptide (16) do not require active translation for decay and appear to be stabilized by polysomes. Hua and Hod (13) have proposed that these messages exist in two pools, a translated polysome compartment that is not subject to decay and a polysome-free compartment that is susceptible to decay.

Although regulation of lipogenic enzymes is mostly transcriptional, message stability clearly participates in the regulation of hepatic lipogenesis. Understanding its role in FAS regulation could provide insight into the mechanisms of hypertriglyceridemia, a condition commonly associated with hyperglycemia. In hopes of clarifying the mechanisms of regulated FAS mRNA stability, we have characterized the 3′ terminus of the FAS message and analyzed FAS message decay after glucose deprivation.

EXPERIMENTAL PROCEDURES

FAS cDNA cloning

Sequencing of both strands of positive clones was performed using Sequenase. A 2083 bp FAS cDNA was isolated from a Clontech (Palo Alto, CA) oligo-dT primed human breast library as described in reference 4. However, this clone did not contain a polyadenylation signal or a poly(A) tract so an oligo-dT-primed HepG2 cDNA library was constructed in λgt22A using the SuperScript System (Gibco BRL, Gaithersburg, MD) to identify the authentic 3′ terminus of the message. The library was screened using standard techniques with a 0.9 kb Sac I/Tth 111 I fragment (nucleotides 589 to 1509 as numbered in Fig. 1), and four independent overlapping clones representing the 3′ terminus of the FAS message were identified. Sequences shared between the clones of HepG2 origin and the human breast cDNA (approximately from bases 1140 to 2080 as numbered in Fig. 1) were identical.

Chromosomal localization

For the human FAS gene, DNA from human/rodent somatic cell hybrid cell lines (BIOS Laboratories, New Haven, CT) was screened by PCR. Four sets of oligonucleotide primers were designed based on the intron-exon organization of the rat gene (17), and the primer pair yielding the strongest specific signal in human DNA was used for screening. PCR was carried out using the upstream primer (nucleotides 55 to 74 of Fig. 1) and downstream primer (the complement of nucleotides 261 to 242 of Fig. 1) with 100 ng of template DNA, in a 10 μl total volume solution containing 10 mM Tris-HCl (pH 8.6), 100 mM KCl, and 3.5 mM $MgCl_2$. The cycling parameters were 94°C/1.5 min for 1 cycle; 94°C/1 min, 60°C/1 min, 72°C/1 min for 30 cycles; and 72°C/4 min for 1 cycle. Products were separated on 2% agarose gels.

Localization of the mouse FAS gene was accomplished by identifying a DNA sequence polymorphism in the gene, and using this polymorphism to genotype the progeny from a backcross of inbred mouse strains. The following compatible primers were synthesized based on available partial mouse FAS cDNA sequence (18): mFAS1 5′ ATG GAG TCG TGA AGC CCC TCA AGT G, mFAS2 5′ GGT CTT GGA GAT GGC AGA AAT CAG G, mFAS3 5′ CGT CTC CAC TCC CGA ATG TGC TT, mFAS4 5′ TCT CCA GCA TGG CAT CCC TCA AAC C. PCR was carried out with mFAS1 and mFAS4 using 200–400 ng of mouse genomic DNA from C57Bl/6J, *Mus m. musculus* Czech II, and *Mus spretus* under standard conditions. These primers are separated by 482 bp in the mouse cDNA but yield a distinct ~900 bp product after PCR using mouse genomic DNA as template, consistent with the presence of an intron. Products were characterized by cycle-sequencing using primers (mFAS2 and 3) internal to the primers used for PCR amplification. A distinct sequence polymorphism extending 3′ from exon 33 (numbered based on the rat gene, ref. 17) was identified and the following strain-specific oligonucleotides were synthesized for allele-specific hybridization and mapping studies: mFASB6 5′ TTC TAG GAT GGG CTG CA, mFASCZ 5′ TTC TAG GAA GGG CTG CA. Simple sequence length polymorphism (SSLP) primers were obtained from Research Genetics (Huntsville, AL). Dinucleotide SSLP polymorphisms were identified for MMU 11 loci using genomic DNA prepared from parental and F_1 animals. Primer se-

quences, cycling parameters, and magnesium concentrations were as specified elsewhere (19).

Using MMU 11 SSLP markers and the FAS PCR-based polymorphism, each locus was analyzed in pairwise combinations for recombination frequencies between each loci and relative order was determined by minimizing double crossover events. Mapping analysis of intersubspecific backcross haplotypes was performed using the computer program Map Manager v 2.5 (20).

Quantitation of FAS mRNA

A human Multiple Tissue Northern blot was obtained from Clontech and probed simultaneously with random-primed human FAS and human γ-actin cDNAs according to instructions provided with the blot. Human tissues were obtained under protocols approved by the Washington University Human Studies Committee. For RNase protection analyses of human message, RNA was prepared as described (4) except for adipose tissue which was isolated as described in reference 21. To generate a human FAS RNA probe, an EcoRI/SacI fragment (nucleotides 1–381 as numbered in Fig. 1) of the human cDNA was subcloned into pGEM-3Z. This plasmid was linearized with EcoRI, in vitro transcription was driven with Sp6 to yield an antisense probe, and protection assays were performed under conditions of probe excess (22). In preliminary experiments, the protection assay for human FAS mRNA was shown to be linear over the range of input RNA used in these studies. The γ-actin probe was generated as described (22).

HepG2 culture conditions and determination of cell viability

Cells were cultured in 100-mm diameter tissue culture dishes as described (4). Briefly, cells were fed RPMI 1640 + 10% FBS + 4500 mg/l D-glucose 4 days after passage to 100-mm dishes. Twenty-four hours later, cells were washed and the media were replaced with RPMI 1640 + 3% BSA + 4500 mg/l D-glucose. Exactly 6 h later (t = 0), cells were washed again and fed RPMI 1640 + 3% BSA + 4500 mg/l D-glucose for the + glucose condition. For the minus glucose condition, cells received RPMI 1640 + 3% BSA containing either water or 4500 mg/l L-glucose.

For determination of viability, cells were plated to 12-well cluster dishes at the same density used for 100-mm diameter dishes. The same feeding protocol described in the preceding paragraph was followed except that some cluster dishes were harvested and assayed for cell viability and DNA content (determined by fluorometry) just before removal of serum. Viability was tested using (3-[4,5-dimethylthiazol-2-yl]-2,5-diphenyl tetrazolium bromide) or MTT in kit form purchased from Sigma. MTT was sterilely reconstituted in RPMI-1640 and 0.1 ml was added to cluster wells containing 1.0 ml of media. Clusters were incubated at 37°C for 2 h, then the purple formazan crystals formed from MTT cleavage by mitochondrial dehydrogenases of living cells were dissolved using acidified isopropanol. MTT cleavage was quantitated spectrophotometrically by absorbance at 570 nm. Each assay included blanks generated from cluster wells containing culture medium without cells.

Characterization of polysomes in density gradients

Message was analyzed in sucrose gradients essentially as described in reference 12. Four to six 100-mm plates of 50–70% confluent HepG2 cells were harvested for each condition at each time point. Cells were placed on ice, washed twice with cold phosphate-buffered saline containing 100 μg/ml cycloheximide, and lysed with 200 μl per dish of lysis buffer (12). Lysates were passed three times through a 27-gauge needle, then nuclei were removed by centrifugation at 12,000 rpm for 3 min at 4°C in a microcentrifuge. Supernatants were layered over linear 15–45% sucrose gradients. Gradients were prepared immediately before use in 100 mM KCl, 5 mM $MgCl_2$, 10 mM HEPES (pH 7.4) using a Jule Inc. (New Haven, CT) gradient mixer and were centrifuged at 40,000 rpm for 1.5 h at 4°C using an SW40 rotor. Fractions (0.5 ml) were collected from the top of the gradients by puncturing the bottom of the tubes and infusing a 50% sucrose solution with a Masterflex pump (model 7518-10, Cole Palmer, Chicago, IL). Fractions were collected in RNase-free glass tubes using a Pharmacia FPLC fraction collector connected to a single-path continuous UV absorbance monitor. Fractions were treated with Proteinase K, extracted with phenol–chloroform, and precipitated; then FAS and γ-actin mRNA levels were assayed by quantitative RNase protection as described above. For experiments involving in vitro release of polysomes with puromycin, lysates were prepared using a high salt buffer (500 mM instead of 100 mM KCl) to maximize polysome release (23). Lysates were then treated with 1 mg/ml puromycin for 30 min at 37°C before density gradient centrifugation for 3 h followed by fractionation and quantitation of message by RNase protection. Complete disruption of polysomes was documented by analysis of UV absorbance tracings in each experiment.

Cell-free FAS mRNA decay

Polysomes and post-nuclear high-speed supernatants (S130) from HepG2 cells were prepared as described in reference 24. Six 100-mm plates at 50–70% density were harvested for each condition. Cells were scraped and suspended in buffer A (10 mM Tris-HCl [pH 7.6], 1.5 mM magnesium acetate, 1 mM potassium acetate, 2 mM

DTT), homogenized using a Dounce homogenizer with a glass pestle, and nuclei were pelleted at 12,000 *g* for 10 min at 4°C. The supernatant was layered over 0.8 ml of freshly prepared buffer B (consisting of 30% w/v sucrose in buffer A) and centrifuged at 39,000 rpm (130,000 *g*) in a Beckman TL-100 ultracentrifuge using a TLS-55 rotor for 2.5 h at 4°C. The supernatant (denoted S130), which had a volume of 1.1–1.3 ml from six dishes of starting material, was removed and stored in aliquots at −70°C. The polysomal pellets were gently resuspended in 0.25 ml of buffer A and stored in aliquots at −70°C. Ribosomal RNA integrity was routinely monitored by electrophoresing small aliquots of polysome preps in ethidium bromide-containing agarose gels; 28S and 18S RNAs of the appropriate intensities were visualized before using polysomes in decay reactions.

For cell-free decay reactions, polysome preps were normalized to the same concentration of RNA using buffer A. Reactions were performed in 1.5-ml sterile microfuge tubes with 10 μl polysomes and 40 μl S130 in a total reaction mixture volume of 83 μl containing the same components described in reference 24. Reactions were started by adding polysomes, carried out for various times at 37°C, then stopped by the addition of urea lysis buffer (7 M urea, 2% SDS, 0.35 M NaCl, 10 mM EDTA, 10 mM Tris-HCl [pH 7.5]). Each assay included t = 0 tubes processed identically except that urea lysis buffer was added before the polysomes to prevent decay. After urea lysis buffer addition, mixtures were extracted with phenol–chloroform and chloroform, RNA was precipitated, and FAS and actin messages were quantitated by RNase protection.

RNase H mapping

Total RNA (20–50 μg per tube) in a volume of 10 μl of water was made 1 mM in EDTA, heated to 100°C for 5 min, then placed on ice. A specific oligonucleotide (0.5 μg) complementary to the message or the same amount of oligo-dT was added to each tube. For FAS mRNA, RNase H cleavage was directed by an oligonucleotide complementary to nucleotides 1740 to 1721 in Fig. 1. For γ-actin, the oligonucleotide 5′ TCT TTT CGA AGG CTT ATT CC, complementary to positions 1320–1301 of the message as numbered in GenBank (Accession M24241), was used to direct cleavage. After 10 min at room temperature each tube was made 50 mM in KCl, and the tubes were incubated for an additional 10 min at room temperature. The samples were made 20 mM in Tris-HCl (pH 7.5), and 28 mM $MgCl_2$ in a total volume of 50 μl, and 1–2 units of RNase H was added to each sample. After incubation at 37°C for 30 min, samples were extracted once with phenol–chloroform, precipitated, and subjected to Northern blotting. Blots were probed with random-primed cDNA fragments 3′ of the RNase cleavage site (for FAS, a fragment extending from ~nucleotides 1785 to 2083 in Fig. 1; for γ-actin, a HindIII/XbaI fragment extending from ~nucleotides 1332 to 1599 as numbered in GenBank), washed under conditions of high stringency, and autoradiographed for 2–9 days.

RESULTS

The sequence of the 3′ terminus of the human FAS message is shown in **Fig. 1.** FAS adds two carbon fragments to a growing acyl backbone anchored by a phosphopantetheine group to the acyl carrier protein region. Once the acyl chain reaches 16 carbons, it is released by the FAS thioesterase to yield free palmitate. The acyl carrier protein region and the thioesterase region are denoted by boxes. The predicted amino acid sequences of these regions are compared to those published for other species (25 [and references therein], 26–35) in **Fig. 2.** At the putative thioesterase active site, the sequence GYSYG was present in human, rabbit, and pig, consistent with the GXSXG motif characteristic of serine hydrolases.

The coding region of the human FAS message was 81% homologous at the nucleotide level to the corresponding region of the rat message. The human 3′ untranslated region (806 nucleotides) was only 59% homologous to the corresponding region for rat (36) but did contain two regions with higher degrees of homology (**Fig. 3A**). AUUUA regions #1 (82% homology) and #2 (88% homology) each contained an AUUUA motif and were AU-rich. The entire human 3′ untranslated region was 37% AU/63% GC; AUUUA region #1 was 59% AU/41% GC and region #2 was 66% AU/34% GC. Curiously, the human message also contained a potential stem–loop structure overlapping region #2 that was similar to an iron-responsive element or IRE (Fig. 1 and Fig. 3B).

The human FAS gene was localized by screening DNA from 20 human/rodent hybrid cell lines by PCR as described in Experimental Procedures. Primers amplified a 207 bp fragment in cloned cDNA, human genomic DNA, and in hybrid lines containing chromosome 17 (**Fig. 4**), making this chromosome 0% discordant (**Table 1**). The same assay was used to screen miniprep DNA prepared from YAC clones representing human chromosome 17 (a gift from Drs. M. Behlke and D. Page, Boston) and FAS signal was detected in a single ~240 kb clone (not shown) mapping to 17q24-25. These data confirm those of another group that recently localized human FAS to 17q25 (37).

The mouse gene was mapped to distal chromosome 11, syntenic for human 17q. Mapping was determined

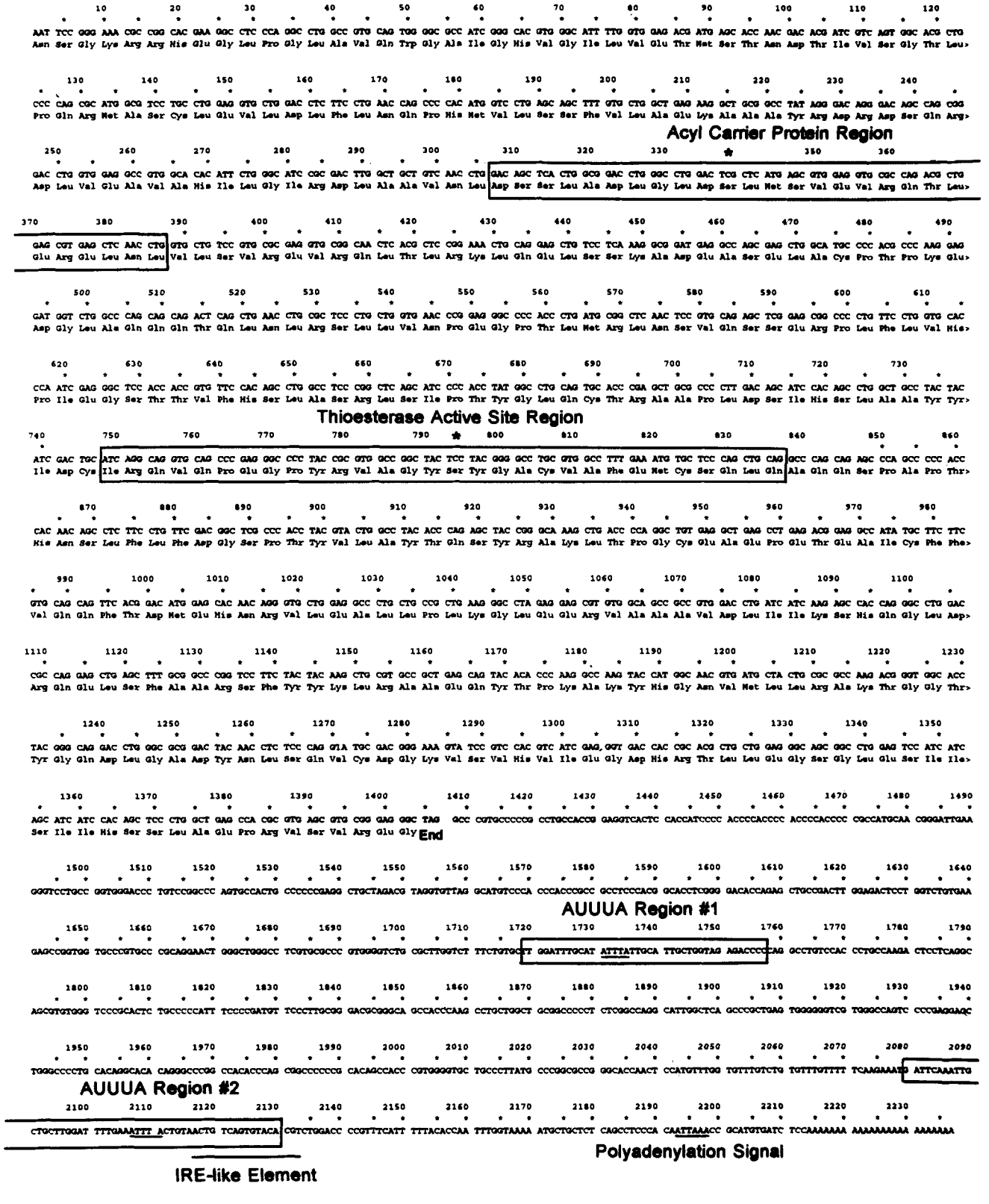

Fig. 1. Nucleotide and predicted amino acid sequence of the 3′ terminus of the human FAS mRNA. The putative acyl carrier protein (with the attachment site of the phosphopantetheine group indicated by an asterisk) and thioesterase active site (with the postulated active site serine indicated by an asterisk) are denoted in the coding region by boxes. AUUUA regions #1 and #2, relatively AU-rich regions containing an AUUUA motif that is underlined, are denoted by boxes in the 3′ untranslated region. At the bottom of the figure, an IRE (iron-responsive element)-like element as well as the putative AUUAAA polyadenylation signal are underlined.

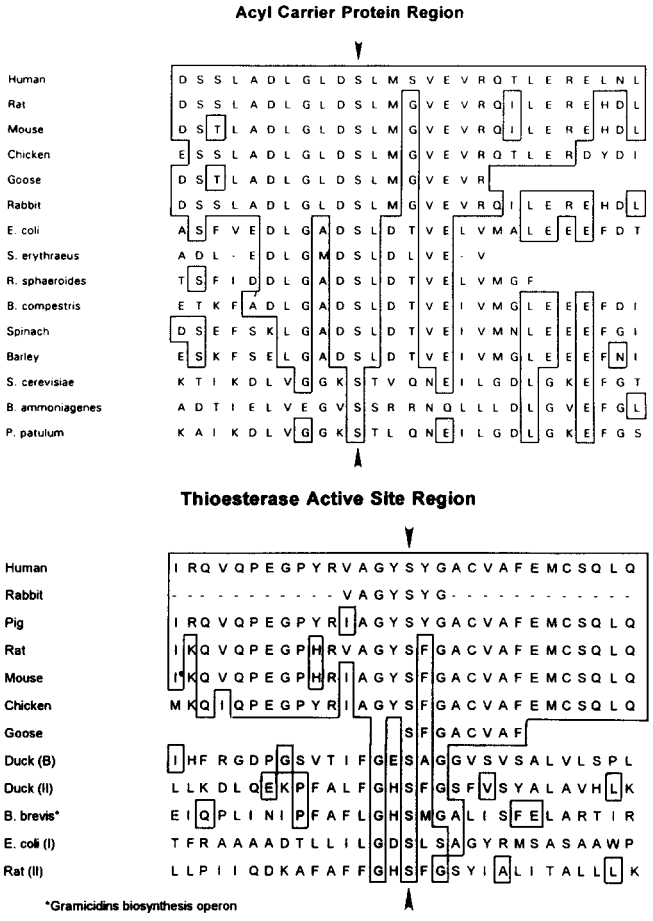

Fig. 2. Comparison of known amino acid sequences for different species at the acyl carrier protein (top) and thioesterase active site (bottom). Human sequences correspond to the coding region boxes indicated in Fig. 1. Arrowheads denote the serine residues identified by an asterisk in Fig. 1.

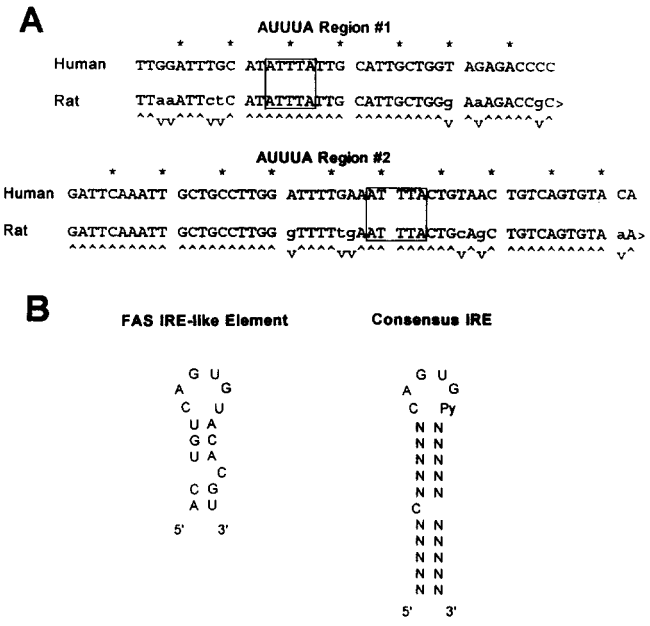

Fig. 3. AUUUA regions and an IRE-like element in the 3′ untranslated region of the human FAS mRNA. In panel A, AUUUA regions #1 and #2, as identified in Fig. 1, are compared to the same regions of the rat FAS mRNA with the shared AUUUA motifs denoted by boxes. In panel B, the predicted stem–loop structure of the IRE (iron-responsive element)-like element in the human mRNA, as identified in Fig. 1, is compared to the consensus sequence for an IRE.

by intersubspecific backcross analysis using progeny derived by mating (C57Bl/6J X *Mus m. musculus* Czech II) F_1 females to C57Bl/6J males (38). All N_2 progeny were genotyped for MMU 11 markers as C57Bl/6J homozygous (BB) or C57Bl/6J X *Mus m. musculus* Czech II heterozygous (BZ) using SSLP and ASO analyses as described in Experimental Procedures. Representative ASO blots are shown in **Fig. 5,** panel A, the haplotypes for all N_2 progeny are shown in panel B, and a genetic linkage map of the distal mouse chromosome 11 based on these data is shown in panel C. The calculated map distances ± SEM between adjacent loci are (centromere), I15, 20.3 ± 3.2, D11Mit32, 12.0 ± 2.6, D11Mit11, 1.9 ± 1.1, D11Mit104, 0.6 ± 0.6, Fasc, (telomere).

RNA blotting using an FAS cDNA showed the FAS message (~9.3 kb) to be expressed in all human tissues studied with the highest levels in lung and liver (**Fig. 6**). Using a fragment of the FAS cDNA as template, an FAS RNA probe was generated that also detected a 9.3 kb message by Northern blotting with HepG2 cell RNA (**Fig. 7,** panel A). This RNA probe protected FAS message in human skeletal muscle, intra-abdominal adipose tissue, and HepG2 cells (panel B). Using in vitro transcribed FAS sense cRNA to generate a standard curve, FAS message was quantitated in HepG2 cells, muscle, and intra-abdominal fat from two separate individuals (panel C). Human adipose tissue is not thought to be a major site of lipogenesis (39), instead serving as a repository for fat synthesized elsewhere. But if one standardizes FAS message in Figs. 6 and 7/panel C based on muscle mRNA levels, HepG2 cells and human liver contain similar amounts of FAS message, and FAS expression in human intra-abdominal fat is surprisingly high. We previously used RNA blotting to show that glucose regulates FAS mRNA levels (4). RNase protection (Fig. 7, panel D) confirmed this finding, and demonstrated that glucose had the same quantitative effect on FAS message whether isolated first as total RNA or after fractionation as polysomes.

RNase protection was used to study the kinetics of FAS mRNA decay after glucose deprivation (**Fig. 8**). Transcription run-off experiments within this time frame show no differences in FAS transcription but do show increases in actin transcription in the absence of glucose (4). The lack of detectable differences in FAS

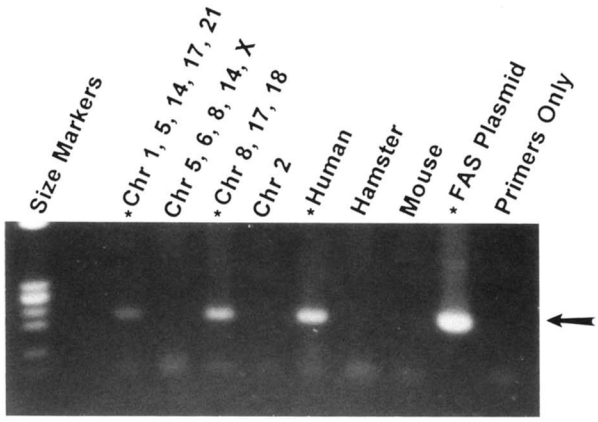

Fig. 4. Localization of the human FAS gene to chromosome 17. Polymerase chain reaction was performed on genomic DNA from human/rodent somatic cell hybrid cell lines using oligonucleotide primers based on sequence in Fig. 1. The predicted 207 base pair amplification product (denoted by an arrow) was amplified from reactions (denoted by an asterisk) using chromosome 17-containing cell lines, human genomic DNA, and a cloned human FAS cDNA, but not from cell lines without chromosome 17, hamster or mouse DNA and not from reactions in which DNA was omitted ("primers only" lane). For the hybrid with chromosomes 1, 5, 14, 17, and 21, only 30% of the cells included chromosome 17 compared to 100% for the line with chromosomes 8, 17, and 18, which may explain the difference in signal intensities.

TABLE 1. Discordance analysis for the human FAS gene

	Concordant		Discordant		
Chromosome	+/+	−/−	+/−	−/+	% Discordance
1	1	15	1	3	20
1	1	15	1	3	20
2	0	17	2	1	15
3	0	16	2	2	20
4	0	16	2	2	20
5	1	5	1	13	70
6	0	16	2	2	20
7	0	16	2	2	20
8	1	16	1	2	15
9	0	17	2	1	15
10	0	17	2	1	15
11	0	17	2	1	15
12	0	16	2	2	20
13	0	13	2	5	35
14	1	13	1	5	30
15	0	16	2	2	20
16	0	16	2	2	20
17[a]	2	18	0	0	0[a]
18	1	15	1	3	20
19	0	12	2	6	40
20	0	16	2	2	20
21	1	14	1	4	25
22	0	16	1	3	20
X	0	16	2	2	20
Y	0	15	2	3	25

Genomic DNA from human/rodent somatic cell hybrid cell lines was screened by polymerase chain reaction using oligonucleotide primers based on the sequence in Fig. 1 as described in Experimental Procedures.

[a]Representative assay results for the two DNA samples scored as positive for the 0% discordant chromosome (17) are shown in Fig. 4.

transcription makes it likely that panel A of Fig. 8 represents mostly the effects of glucose on message decay and not a balance between synthesis and degradation. FAS message decay after glucose deprivation (panel A, open circles) was complicated, consisting of a slow decay phase (first 2–4 h), a period of more rapid decay (6–10 h), then a plateau phase (12–18 h). Actin message (panel B) increased when glucose was removed.

Analyses were also performed on cells treated with the transcription inhibitor DRB (dichloro-ribofuranosylbenzimidazole), under conditions shown in preliminary experiments to decrease newly synthesized cytoplasmic message by 85–90%. FAS mRNA decayed more rapidly after glucose deprivation (panel C) and reached the same plateau phase seen in the absence of transcription inhibition (panel A). However, transcription inhibition decreased the time required to reach this plateau (6 h with DRB vs. 12 h without DRB, compare panels A and C). As expected, DRB prevented the increase in actin message after glucose deprivation (panel D).

To verify that the accelerated decay of FAS mRNA after glucose deprivation in serum-free media did not simply represent cell death, HepG2 cell viability was documented using MTT, cleaved by mitochondrial dehydrogenases of living cells, as described in Experimental Procedures, and by quantitating DNA content. As shown in **Table 2,** both MTT cleavage products and DNA content were actually higher for cells cultured in serum-free media without glucose as compared to parallel dishes containing serum that were harvested 18 h earlier. There were no differences between + and − glucose conditions in serum-free media. These data indicate that HepG2 cells are viable under our experimental conditions. Others have also shown that HepG2 cells are unaffected by culturing for up to 24 h in serum-free media (40).

The sedimentation of FAS message in density gradients was also studied by RNase protection. A typical polysome profile is shown in **Fig. 9,** panel I. Glucose deprivation (L-glucose treatment) was associated with a shift in ribosomal RNA toward lower densities indicating a decrease in the number of polyribosomes (fractions 6–16) and an increase in monosomes (fractions 4–5). The profile shown represents cells treated for 3 h but identical patterns persisted for 12 h after feeding. If message is associated strictly with polysomes, it should shift toward lower densities after L-glucose treatment. However, if a polysome-independent mRNA compartment exists, message in this compartment would sediment independent of polysomes and not necessarily shift toward lower densities.

Consistent with the existence of such a compartment, a fraction of the FAS message was retained in the dense region of gradients after glucose deprivation for 3 h,

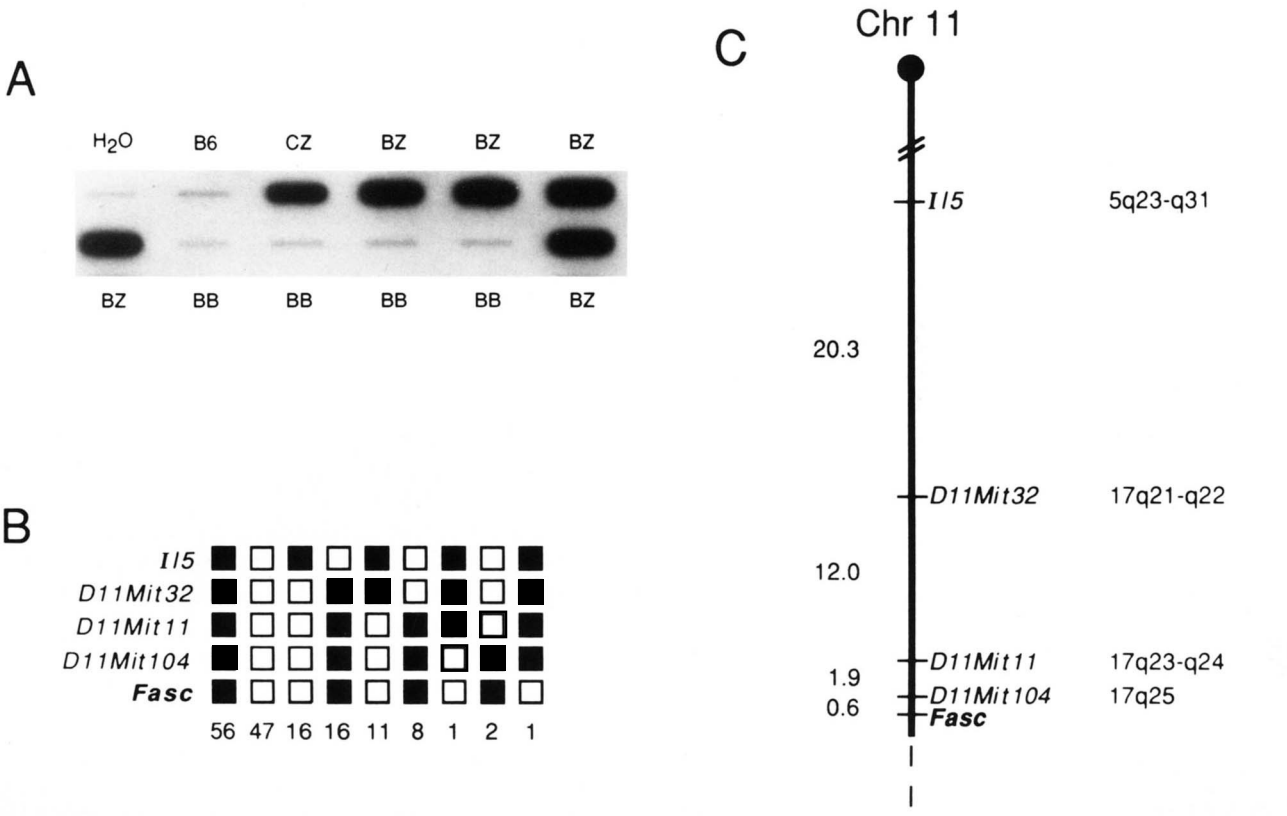

Fig. 5. The Fasc locus (Fasc) maps to the distal region of mouse chromosome 11 (MMU 11). Panel A shows an allele-specific oligonucleotide (ASO) hybridization analysis of the mouse Fasc gene. PCR amplification was performed on a water control (H_2O), genomic DNA from C57Bl/6J (B6) and *Mus m. musculus* Czech II mice (CZ), and genomic DNA from 9 representative intersubspecific backcross progeny. ASO hybridization was conducted using an oligonucleotide (mFASCZ) hybridizing specifically to the PCR product generated from *Mus m. musculus* Czech genomic DNA. Genotype scoring of each PCR sample is indicated above or below the slot blot as BB (homozygous C57Bl/6J) or BZ (heterozygous C57Bl/6J X *Mus m. musculus* Czech II). Panel B shows haplotype data. The segregation patterns of Fasc and proximal loci in a C57Bl/6J X (C57Bl/6J X *Mus m. musculus* Czech II) F1 intersubspecific backcross that were typed for all loci in all 158 backcross animals are shown. Each column represents the chromosome identified in the backcross progeny that was inherited from the (C57Bl/6J X *Mus m. musculus* Czech II) F1 parent. Shaded boxes represent the presence of a *Mus m. musculus* Czech II allele and open boxes represent the presence of a C57Bl/6J allele. The number of offspring inheriting each type of chromosome is listed at the bottom of each column. For panel C, a partial chromosome 11 linkage map showing the position of Fasc in relation to proximal loci is shown. Recombination distances between loci in centimorgans (1 cM = 1% recombination) are shown to the left of the chromosome and the positions of loci in human chromosomes are shown to the right.

causing L-glucose (broken line) and D-glucose (solid line) FAS message profiles to co-migrate in fractions 9–16 (Fig. 9, panel IIA). This retention was transient, because at 6 and 12 h (panels B and C) FAS message shifted toward lower densities. Actin message was not retained in the dense region at 3 h (compare fractions 9–16 of panels A and D) instead shifting toward lower densities in parallel with the polysome shift (see arrowheads in panel D which denote shifted fractions).

The retention of FAS mRNA in the dense region at 3 h and shift of actin mRNA toward lower densities at 3 h was a consistent observation. Changes were not due to variability in polysome preparations; every gradient was monitored by continuous UV absorbance at 254 nm and showed consistent profiles (Fig. 9, panel I). By quantitating peak heights in the fractions (6–12) to which messages shifted after glucose deprivation, statistically significant differences were demonstrated between glucose conditions for actin and but not FAS mRNA. In three independent experiments at 3 h, the actin message shifted to lower densities after glucose deprivation (P = 0.0290 by comparing D-glucose and L-glucose peak heights in fractions 6–12 by paired two-tailed t test) while the FAS message did not (P = 0.3937).

If the statistically significant, transient retention of FAS message in the dense region of gradients is caused by a polysome-independent compartment, releasing ribosomes from message with puromycin in vitro should not affect the more rapid sedimentation of the FAS message. Consistent with this model, glucose depriva-

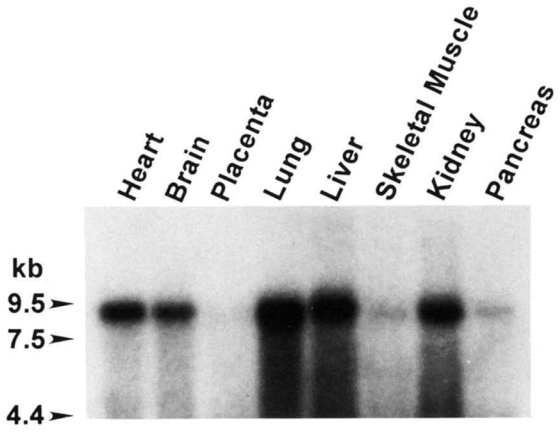

Fig. 6. Determination of expression of the FAS mRNA in human tissues by Northern blotting. A commercially available blot was probed with a human FAS cDNA. A single 9.3 kb FAS mRNA species was seen in all tissues (including placenta, the signal for which was clearly visible on longer exposures). A γ-actin cDNA was included in the hybridization and showed essentially the same level of expression of the 2.1 kb actin message in all tissues (not shown in this photograph due to the higher levels of expression of actin). Only the 9.3 kb FAS and 2.1 kb γ-actin bands were seen in each lane, except for the lane containing RNA from pancreas which also showed a 3.0 kb species of uncertain significance.

tion for 3 h caused a fraction (arrowheads in inset, panel IIA) of the FAS mRNA to sediment more rapidly than + glucose message after polysome disruption, a pattern not seen for actin (not shown).

The detection of polysome-independent migration associated with accelerated message decay suggests that polysomes protect FAS mRNA from decay. To test this hypothesis, polysome profiles were generated from cells cultured for 12 h with or without D-glucose in the presence of translational inhibitors (**Fig. 10**) under conditions previously shown to decrease protein synthesis by ~90% (4). Unlike Fig. 9 where data were normalized to the peak fraction in each profile, data in Fig. 10 were not normalized in order to determine how different translational inhibitors affect the decrease in FAS mRNA with glucose deprivation. Puromycin, an inhibitor of translation initiation that releases message from polysomes, had no effect on the accelerated decay of FAS message after L-glucose treatment (panels A and D), but cycloheximide, an elongation inhibitor that promotes the association of message with polysomes, blocked L-glucose-associated decay (panels B and E). In panel E note the decrease in the size of the monosome peak (~fraction 5) and the relative increase in the polysome fractions consistent with the immobilization of ribosomes on message induced by cycloheximide. The cycloheximide effect was not independent of the polysome effects of this agent as L-glucose-associated accelerated decay occurred when cells were cultured with both puromycin and cycloheximide (panels C and F).

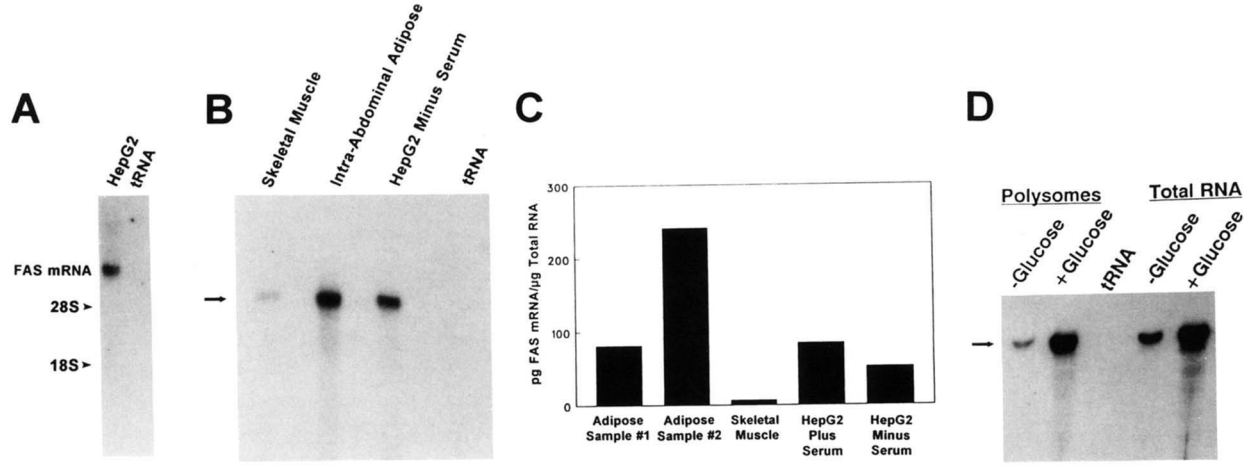

Fig. 7. Ribonuclease protection of human FAS message. A uniformly labeled human FAS RNA probe was generated by in vitro transcription. Panel A shows that this probe detects the 9.3 kb FAS message by Northern analysis of 15 µg of HepG2 total RNA without reacting with the same amount of yeast tRNA. Panel B shows that this FAS RNA probe protects a fragment of the predicted size (~381 nucleotides as indicated by the arrow) in 10 µg aliquots of total RNA from human skeletal muscle, human intra-abdominal adipose tissue, and HepG2 cells but does not react with the same amount of tRNA. Panel C shows the results of a quantitative assay of FAS mRNA performed by comparing the results of RNase protection of unknowns (human RNA) with a standard curve generated using counts from known amounts of in vitro transcribed sense FAS mRNA. Data represent the mean of duplicate determinations for the two adipose tissue samples and the muscle sample, and the mean ± SEM for the HepG2 samples (with error bars too small to be seen). Separate aliquots of "Adipose Sample #1" and "HepG2 Minus Serum" RNA were used for the gel shown in panel B. For panel D, HepG2 cells were cultured in the presence or absence of glucose for 12 h followed by preparation of total RNA or isolation of polysomes followed by RNase protection using the FAS RNA probe.

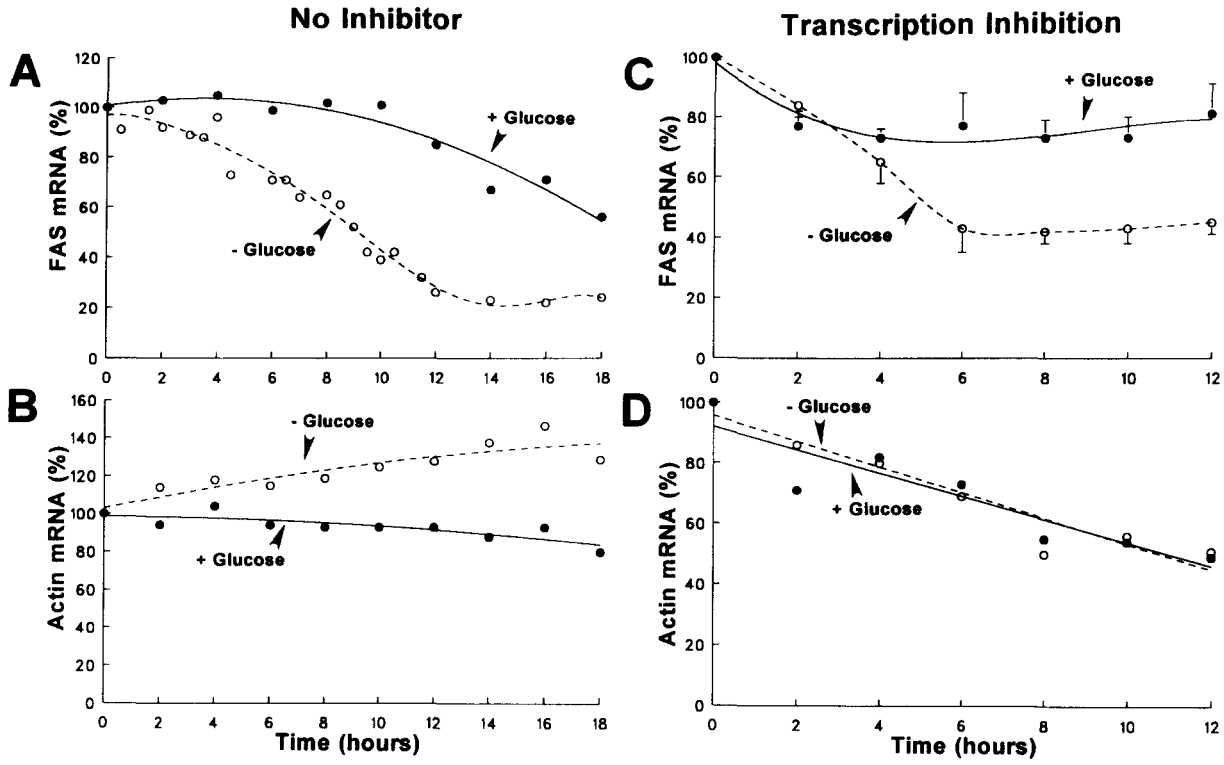

Fig. 8. Kinetic analysis of FAS and γ-actin mRNA in HepG2 cells after + or – glucose feeding. As described in Experimental Procedures, HepG2 cells were fed serum-free medium with (solid line, closed symbols) or without (broken line, open symbols) D-glucose at time 0 followed by isolation of total RNA and determination of human FAS mRNA (panel A) and human γ-actin mRNA (panel B) by quantitative RNase protection assay. Hybridizations were performed using amounts of total RNA yielding signals within the linear response range for each assay. Similar results were obtained in three independent experiments. For panels C and D, the same analyses were performed in the presence of the transcription inhibitor DRB (dichloro-ribofuranosylbenzimidazole, 65 μM). For panel C, data represent the mean ± SEM of determinations from three independent experiments; the + and – glucose values at 12 h were significantly different ($P = 0.0323$).

In order to provide direct evidence for an mRNA degradation system, we prepared polysomes and post-nuclear high-speed supernatants from cells cultured with or without glucose and studied message decay in a cell-free assay (**Table 3**) as described by Brewer and Ross (24). Preliminary experiments revealed progressive decreases in both FAS and actin mRNA over time with both messages completely degraded by 3 h. Additional

TABLE 2. HepG2 cell viability in the absence of serum and glucose

Culture Conditions	MTT Cleavage (absorbance at 570 nm)	DNA (micrograms/well)
1. RPMI-1640 + 10% FBS with glucose	2.505 ± 0.063	7.1 ± 0.81
2. RPMI-1640 + 3% BSA with glucose	3.074 ± 0.008	15.6 ± 0.62
3. RPMI-1640 + 3% BSA without glucose	3.043 ± 0.008[a]	15.8 ± 0.80[b]

HepG2 cells were plated to 12-well cluster dishes in MEM + 10% FBS on day 1. On day 4, media were replaced with RPMI-1640 + 10% FBS with glucose as described in Experimental Procedures. On day 5, one third of the clusters (culture condition 1) were harvested and assayed for living cells using MTT as described in Experimental Procedures. DNA content for each well was determined fluorometrically using a Hoeffer TKO DNA Fluorometer. The remaining cells were washed with phosphate-buffered saline and fed RPMI-1640 + 3% BSA with 4500 mg/l D-glucose. Six hours later, cells were washed again; then half received RPMI-1640 + 3% BSA with 4500 mg/l D-glucose (culture condition 2) and half received the same media without glucose (culture condition 3). Twelve hours later, cells were assayed for viability and DNA content. For this representative experiment, values represent mean ± SEM for six wells. The same results were seen in a total of three independent experiments.

[a] $P < 0.0001$ vs. Condition 1; not significant vs. Condition 2.

[b] $P < 0.0001$ vs. Condition 1; not significant vs. Condition 2.

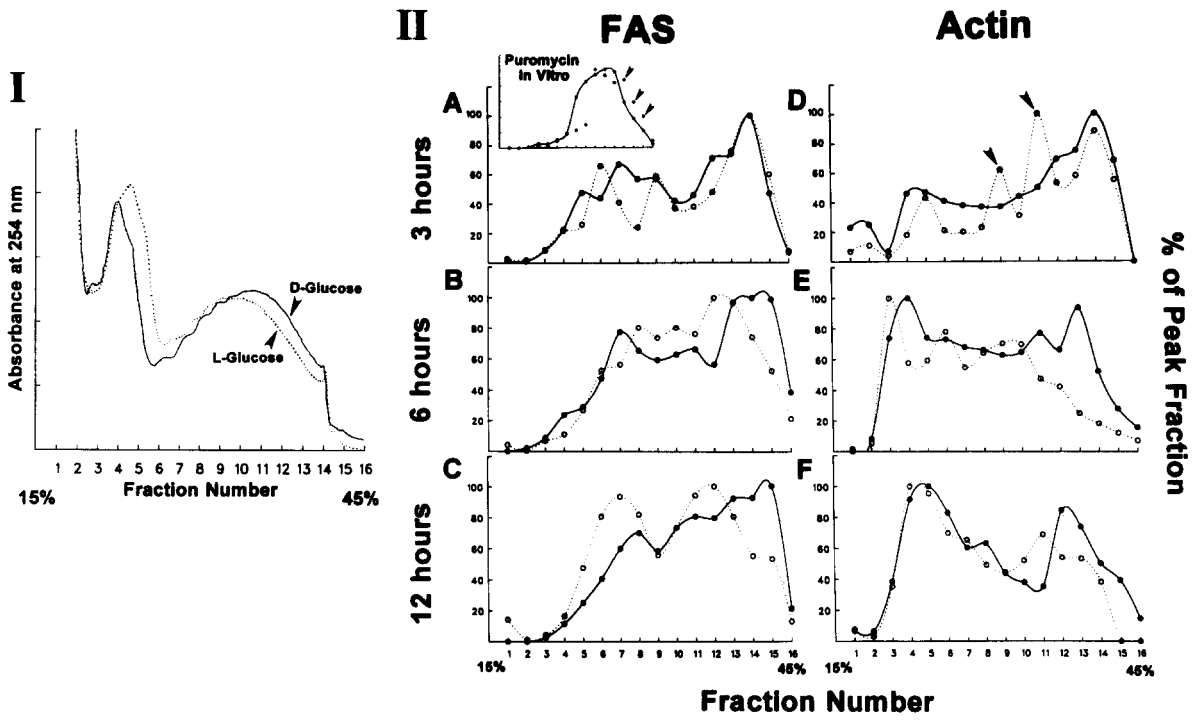

Fig. 9. FAS but not actin message is transiently retained at the high density region of sucrose gradients after glucose deprivation. Panel I shows a representative polysomal profile for HepG2 cells after D-glucose or L-glucose feeding. Cells from several dishes were pooled, then cytoplasmic extracts were separated in 15–45% sucrose gradients. Fractions were collected from the top of the gradients (represented by the left side of the panel) and RNA content was monitored continuously as absorbance at 254 nm. This particular profile was obtained with cells at the 3-h time point, but patterns for D- and L-glucose were identical at later time points. Panel II shows the migration of FAS (panels A, B, C) and actin (panels D, E, F) mRNA in sucrose gradients at 3, 6, and 12 h after glucose deprivation. Solid line/closed symbols represent D-glucose and broken line/open circles represent L-glucose. Message in each fraction is expressed as the percentage of the peak fraction in each profile in order to determine the migration positions for messages. The actual amount of the FAS message decreased and actin message increased over time in the presence of L-glucose. Data shown are representative of at least three independent experiments for each time point. Note in panel IIA that the FAS message does not follow the total polysomal shift (see panel I) toward lower densities after glucose deprivation. Actin message does shift (see arrowheads in panel D) toward lower densities at 3 h. In three separate experiments, the actin message shifted (P = 0.0290 by comparing D-glucose and L-glucose peak heights in the shift densities) while the FAS message did not (P = 0.3937). The inset for panel A shows the migration of FAS message in a sucrose gradient after releasing polysomes in vitro with puromycin. A substantial proportion of the FAS message (arrowheads in inset) from L-glucose-treated cells sedimented to a position more dense than message from D-glucose-treated cells in three independent profiles. This pattern was not seen for FAS mRNA at later time points and was not seen for actin (data not shown).

preliminary experiments showed that when magnesium was omitted from reactions, decay did not occur over 1 h, suggesting that our cell-free system does not simply reflect nonspecific ribonucleases which are usually cation-independent (41). As shown in Table 3, glucose deprivation consistently resulted in accelerated decay of FAS but not actin message in cell-free decay assays using both polysomes and cell supernatants.

Finally, the FAS mRNA poly(A) tail was characterized after glucose deprivation (**Fig. 11**). RNase H cleavage was directed by an FAS-specific oligo ~500 nucleotides upstream of the 3′ terminus of the message followed by Northern blotting and detection with a probe downstream of the RNase H cleavage site (panel A). A heterogeneous signal of the expected size [~500–800 nucleotides and representing message with different-sized poly(A) tails] was seen only when RNA was treated with RNase H and the FAS-specific oligo (panel B, lane A). Including oligo-dT in cleavage reactions produced a major band of ~500 nucleotides that defined the non-adenylated 3′ terminus of the message (arrow, lane B of panel B). After 12 h (panel C), there was no difference in poly(A) tail length or heterogeneity between cells cultured with (lanes 1–3) or without (lanes 4–6) glucose. In two of two additional experiments (not shown), RNase H mapping of + and – glucose RNA at two hour intervals for up to 12 h showed no detectable differences in the poly(A) tail. Glucose deprivation also had no detectable effect on poly(A) tail length for the actin message (not shown).

DISCUSSION

FAS is necessary for the endogenous production of fatty acids and understanding its regulation in human

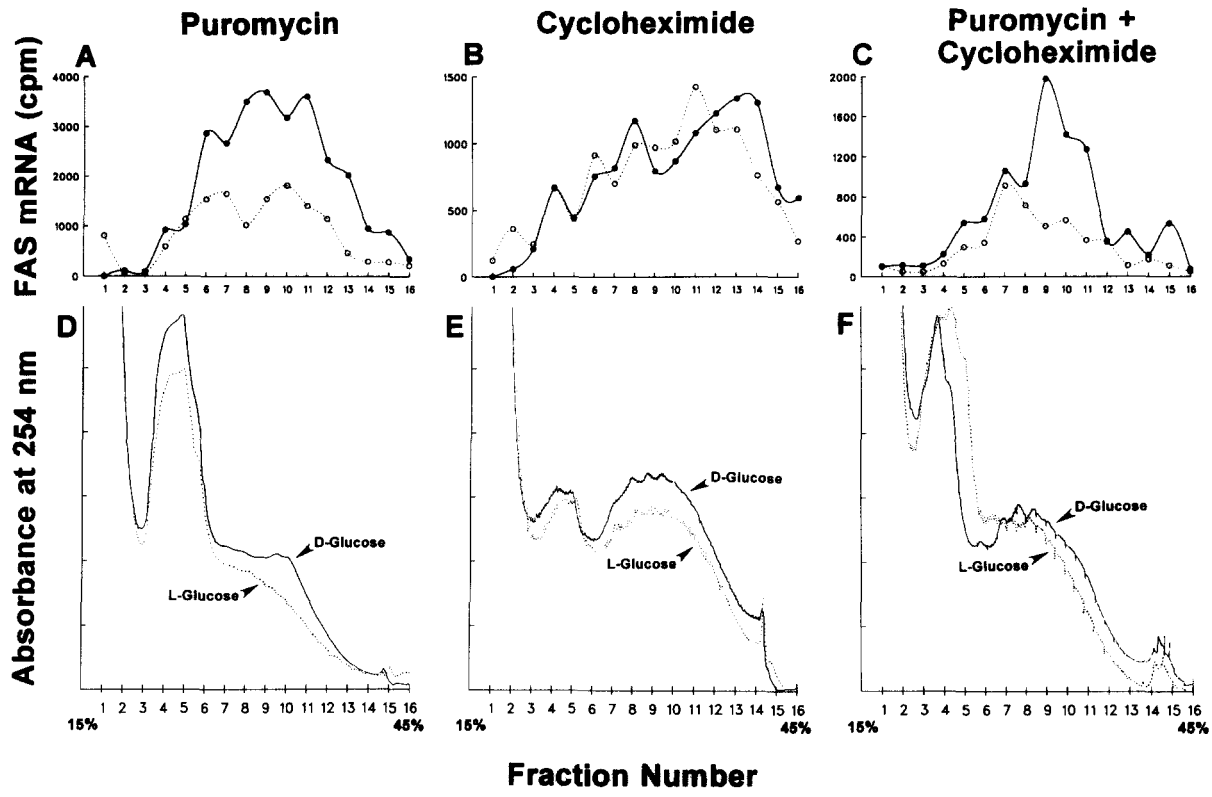

Fig. 10. Association with polysomes prevents accelerated FAS mRNA decay after glucose deprivation. HepG2 cells were subjected to + (solid symbols) and – (open symbols) glucose feeding for 12 h in the presence of puromycin (100 μM, panels A and D), cycloheximide (10 μM, panels B and E), or both (panels C and F). Panels A, B, and C show FAS mRNA levels and panels D, E, and F show the polysomal profile for the experiment depicted immediately above each profile. Unlike Fig. 9, message data for this figure are presented as actual cpm to show that FAS mRNA decays after glucose deprivation when polysomes are disrupted by puromycin (panel A), but not when polysome aggregation is promoted by cycloheximide (panel B). That this effect is not mediated by some ribosome-independent effect of cycloheximide is shown in panel C where accelerated decay is observed after in vivo treatment with both inhibitors. To ensure that data were not biased by differences in polysomal yield, total RNA (without polysomal manipulations) from parallel dishes was assayed and showed the same quantitative differences for FAS mRNA between D- and L-glucose treated cells (not shown).

TABLE 3. Glucose deprivation accelerates cell-free FAS mRNA decay

	mRNA Remaining after in Vitro Decay Reaction (expressed as % of input mRNA)	
	Plus Glucose	Minus Glucose
FAS message	96.4 ± 18%	43.8 ± 12%[a]
Actin message	70.3 ± 10%	86.0 ± 6%[b]

HepG2 cells were cultured as described in Experimental Procedures. Three hours after feeding serum-free media with or without glucose, polysomes and cytoplasmic extracts were isolated from six 100-mm plates per condition as described in Experimental Procedures. In vitro decay reactions were performed at 37°C for 15 min using 100 μg polysomal RNA per reaction tube and the cell equivalent volume of cytoplasmic extract. Results are expressed as mean ± SEM % of FAS or γ actin mRNA (assayed by RNase protection) remaining after cell-free decay compared to the input FAS or γ actin mRNA. Similar results were seen in five independent experiments.

[a]P = 0.0396 vs. plus glucose (n = 5).

[b]P = 0.2142 vs. plus glucose (n = 4).

cells could be relevant to disorders such as obesity, hyperlipidemia, and diabetes mellitus. Consistent with the potentially important role of this protein in human pathophysiology, we show that human FAS expression is high in liver and intra-abdominal fat (Figs. 6 and 7), sites critical to the development of common metabolic diseases. FAS gene expression at both of these sites can be altered by regulated message stability, and in this paper we have characterized the kinetics of FAS mRNA decay in response to glucose deprivation in HepG2 cells.

Message decay is generally thought to be a first order process, but FAS mRNA decay was complicated and included a plateau phase (Fig. 8). These findings are consistent with those older studies showing that message decay occurs by at least two processes with different rate constants (42). Recent studies also suggest that the decay of short-lived messages is not first order (43). Shaw and Kamen (44) reported accelerated decay of a β-globin/GM-CSF 3′ untranslated AU construct that was

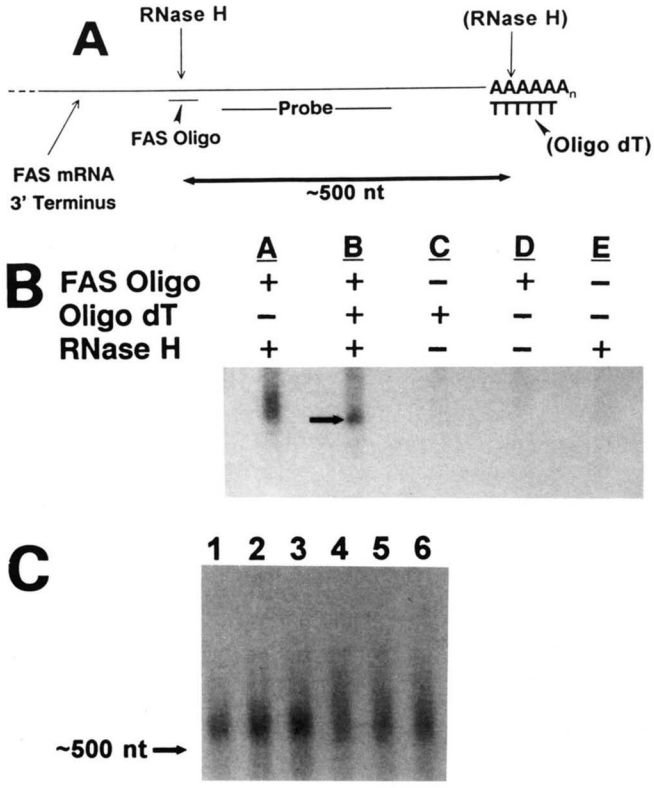

Fig. 11. RNase H mapping of the 3′ terminus of the human FAS message. Panel A shows a schematic diagram of the location of the FAS oligonucleotide used to direct RNase H cleavage of the human FAS message and the region used to generate a probe for detection of the message after RNase cleavage. Panel B shows that detection of the expected 500–800 nucleotide 3′ terminus of the FAS message [with the size range due to the presence of FAS message containing poly(A) tails of differing lengths] depends on the presence of the FAS-specific oligo and RNase H (lane A). For lane B, oligo-dT was included in the reaction to define the non-adenylated terminus of the message, indicated by the arrow. However, a "ladder" of bands with lesser intensity representing message fragments up to ~800 nucleotides long was also seen in lane B, probably caused by the hybridization of oligo-dT at multiple sites in the poly(A) tail. For panel C, HepG2 cells were cultured for 12 h in the presence (lanes 1–3) or absence (lanes 4–6) of glucose followed by preparation of total RNA and RNase H mapping with the FAS-specific oligonucleotide. This blot represents reactions using 20 μg of total RNA (each from separate dishes of cells) for lanes 1–3 and 50 μg of total RNA (each from separate dishes) for lanes 4–6 to compensate for the decrease in FAS mRNA after glucose deprivation. The ~500 nucleotide position indicated by the arrow was determined by including a separate reaction on the same gel in which oligo-dT was included to define the non-adenylated terminus of the message.

not first order and plateaued at 20–30% of initial levels. FAS message also plateaus at ~20% of initial levels, and this occurs between 12 and 18 h after glucose deprivation (Fig. 8). With transcription inhibition, the plateau phase was reached at 6 h instead of 12 and message stabilized at ~40% of initial levels. This suggests that transcription of other species such as antisense RNA (45, 46) may participate in FAS message decay.

FAS message was transiently but consistently retained in the dense region of sucrose gradients during decay, a retention that persisted after release from polysomes (Fig. 9). A similar polysome-independent retention was recently reported for decay of GM-CSF mRNA (12), a message that, like the FAS mRNA, contains 3′ untranslated region AUUUA motifs. Although complete characterization of the cellular components responsible for this retention is beyond the scope of this study, the possibility that this migration represents a cytoplasmic decay compartment is supported by our demonstration of glucose-regulated decay in a cell-free system that included cytoplasmic extracts (Table 3).

We speculate that a common cytoplasmic decay compartment may be shared by several eukaryotic messages. For short-lived messages requiring translation for decay, translation could modify the message in some way necessary to access this compartment. Messages like FAS (Fig. 10), PEPCK (13), tyrosine aminotransferase (14), vitellogenin (15), and vasoactive intestinal polypeptide (16) which do not require translation for decay and are protected by ribosomes, would access this compartment through another mechanism perhaps involving RNA-binding proteins. Several such proteins have been identified (47–50) but direct evidence that these proteins mediate RNA decay is lacking, perhaps because they primarily allow messages to access a decay compartment. Consistent with this model, we have recently used RNA gel retardation assays and UV crosslinking to identify a cytoplasmic protein that binds to the 3′ terminus of the human FAS mRNA and is regulated by glucose (Chua, M. S., and C. F. Semenkovich, manuscript in preparation).

We were unable to detect any consistent difference in poly(A) tail length of the FAS message during decay (Results and Fig. 11). The apolipoprotein II poly(A) tail also does not change during decay (51). Deadenylation is important for the decay of some messages (43, 52), but the exact relationship between mammalian message decay and deadenylation is uncertain. Some messages demonstrate poly(A) shortening not with decay but during the process of mRNA accumulation (53), and mutating AUUUA motifs can retard the rate of message decay without affecting deadenylation (54).

In summary, the human FAS mRNA is expressed at highest levels in liver, lung, and intra-abdominal fat, and contains two 3′ untranslated region AUUUA motifs. Its decay is complicated and transiently associated with ribosome-independent retention in the dense region of sucrose gradients. Association of message with polysomes prevents decay, and glucose deprivation is associated with accelerated decay in a cell-free system

that includes both polysomes and cytoplasmic extracts. As carbohydrate feeding increases message stability for several lipogenic enzymes, characterizing the individual components of FAS message decay could provide insight into the mechanisms of de novo lipogenesis.

We thank Drs. Greg Sicard and Dirk Baumann, Washington University Department of Surgery, for intra-abdominal adipose tissue samples, and Rick Goforth for technical assistance. This work was supported by a Grant-in-Aid from the National Center of the American Heart Association, grants from the Life and Health Insurance Medical Research Fund and the National Institutes of Health (HL47436 and DK44074), and by the Washington University DRTC (NIH 5 P60 DK20579). This work was done during the tenure of an Established Investigatorship from the American Heart Association (to CFS). FTF is a member of the Curriculum of Genetics and Molecular Biology at The University of North Carolina at Chapel Hill.

Manuscript received 28 November 1994 and in revised form 30 March 1995.

REFERENCES

1. Volpe, J. J., and P. R. Vagelos. 1976. Mechanisms and regulation of biosynthesis of saturated fatty acids. *Physiol. Rev.* **56:** 339–417.
2. Hillgartner, F. B., L. M. Salati, and A. G. Goodridge. 1995. Physiological and molecular mechanisms involved in nutritional regulation of fatty acid synthesis. *Physiol. Rev.* **75:** 47–76.
3. Iritani, N. 1992. Nutritional and hormonal regulation of lipogenic-enzyme gene expression in rat liver. *Eur. J. Biochem.* **205:** 433–442.
4. Semenkovich, C. F., T. Coleman, and R. Goforth. 1993. Physiologic concentrations of glucose regulate fatty acid synthase activity in HepG2 cells by mediating fatty acid synthase mRNA stability. *J. Biol. Chem.* **268:** 6961–6970.
5. Xu, Z. X., W. Stenzel, S. M. Sasic, D. A. Smart, and S. A. Rooney. 1993. Glucocorticoid regulation of fatty acid synthase gene expression in fetal rat lung. *Am. J. Physiol.* **265:** L140–L147.
6. Chalbos, D., F. Galtier, S. Emiliani, and H. Rochefort. 1991. The anti-progestin RU486 stabilizes the progestin-induced fatty acid synthetase mRNA but does not stimulate its transcription. *J. Biol. Chem.* **266:** 8220–8224.
7. Moustaid, N., and H. S. Sul. 1991. Regulation of expression of the fatty acid synthase gene in 3T3-L1 cells by differentiation and triiodothyronine. *J. Biol. Chem.* **266:** 18550–18554.
8. Klausner, R. D., T. A. Rouault, and J. B. Harford. 1993. Regulating the fate of mRNA: the control of cellular iron metabolism. *Cell.* **72:** 19–28.
9. Greenberg, M. E., and J. G. Belasco. 1993. Control of the decay of labile protooncogene and cytokine mRNAs. *In* Control of Messenger RNA Stability. J. G. Belasco and G. Brawermann, editors. Academic Press, Inc., San Diego, CA. 199–218.
10. Peppel, K., J. Vinci, and C. Baglioni. 1991. The AU-rich sequences in the 3′ untranslated region mediate the increased turnover of interferon mRNA induced by glucocorticoids. *J. Exp. Med.* **173:** 349–355.
11. Brewer, G., and J. Ross. 1988. Poly(A) shortening and degradation of the 3′ A + U-rich sequences of human c-myc mRNA in a cell-free system. *Mol. Cell Biol.* **8:** 1697–1708.
12. Savant-Bhonsale, S., and D. W. Cleveland. 1992. Evidence for instability of mRNAs containing AUUUA motifs mediated through translation-dependent assembly of a >20S degradation complex. *Genes & Dev.* **6:** 1927–1939.
13. Hua, J., and Y. Hod. 1992. The role of protein synthesis in the decay of phosphoenolpyruvate carboxykinase messenger RNA. *Mol. Endocrinol.* **6:** 1418–1424.
14. Ernest, M. J. 1982. Regulation of tyrosine aminotransferase messenger ribonucleic acid in rat liver. Effect of cycloheximide on messenger ribonucleic acid turnover. *Biochemistry.* **21:** 6761–6767.
15. Blume, J. E., and D. J. Shapiro. 1989. Ribosome loading, but not protein synthesis, is required for estrogen stabilization of *Xenopus laevis* vitellogenin mRNA. *Nucleic Acids Res.* **17:** 9003–9014.
16. Chew, L-J., D. Murphy, and D. A. Carter. 1994. Alternatively polyadenylated vasoactive intestinal peptide mRNAs are differentially regulated at the level of stability. *Mol. Endocrinol.* **8:** 603–613.
17. Amy, C. M., B. Williams-Ahlf, J. Naggert, and S. Smith. 1992. Intron–exon organization of the gene for the multifunctional animal fatty acid synthase. *Proc. Natl. Acad. Sci. USA.* **89:** 1105–1108.
18. Paulauskis, J. D., and H. S. Sul. 1989. Structure of mouse fatty acid synthase mRNA. Identification of the two NADPH binding sites. *Biochem. Biophys. Res. Commun.* **158:** 690–695.
19. Dietrich, W., H. Katz, S. E. Lincoln, H. S. Shin, J. Friedman, N. C. Dracopoli, and E. S. Lander. 1992. A genetic map of the mouse suitable for typing intraspecific crosses. *Genetics.* **131:** 423–447.
20. Manly, K. K. 1993. A Macintosh program for storage and analysis of experimental genetic mapping data. *Mamm. Genome.* **4:** 303–313.
21. Semenkovich, C. F., S. H. Chen, M. Wims, C. C. Luo, W. H. Li, and L. Chan. 1989. Lipoprotein lipase and hepatic lipase messenger RNA tissue specific expression, developmental regulation, and evolution. *J. Lipid Res.* **30:** 423–431.
22. Levy, R. A., R. E. Ostlund, Jr., G. Schonfeld, P. Wong, and C. F. Semenkovich. 1992. Cholesteryl ester storage disease: complex molecular effects of chronic lovastatin therapy. *J. Lipid Res.* **33:** 1005–1015.
23. Blobel, G., and D. Sabatini. 1971. Dissociation of mammalian polyribosomes into subunits by puromycin. *Proc. Natl. Acad. Sci. USA.* **68:** 390–394.
24. Brewer, G., and J. Ross. 1990. Messenger RNA turnover in cell-free extracts. *Methods Enzymol.* **181:** 202–209.
25. Huang, W. Y., J. K. Stoops, and S. J. Wakil. 1989. Complete amino acid sequence of chicken liver acyl carrier protein derived from the fatty acid synthase. *Arch. Biochem. Biophys.* **270:** 92–98.
26. Meurer, G., G. Biermann, A. Schutz, S. Harth, and E. Schweizer. 1992. Molecular structure of the multifunctional fatty acid synthetase gene of *Brevibacterium ammoniagenes:* its sequence of catalytic domains is formally consistent with a head-to-tail fusion of the two yeast genes FAS1 and FAS2. *Mol. Gen. Genet.* **232:** 106–116.

27. Chirala, S. S., R. Kasturi, M. Pazirandeh, D. T. Stolow, W. Y. Huang, and S. K. Wakil. 1989. A novel cDNA extension procedure—isolation of chicken fatty acid synthase cDNA clones. *J. Biol. Chem.* **264:** 3750–3757.
28. Hardie, D. G., K. B. Dewart, A. Aitken, and A. D. McMarthy. 1985. Amino acid sequence around the reactive serine residue of the thioesterase domain of rabbit fatty acid synthase. *Biochim. Biophys. Acta.* **828:** 380–382.
29. Amy, C. M., A. Witkowski, J. Naggert, B. Williams, Z. Randhawa, and S. Smith. 1989. Molecular cloning and sequencing of cDNAs encoding the entire rat fatty acid synthase. *Proc. Natl. Acad. Sci. USA.* **86:** 3114–3118.
30. Mildner, A. M., and S. D. Clarke. 1991. Porcine fatty acid synthase: cloning of a complementary DNA, tissue distribution of its mRNA and suppression of expression by somatotropin and dietary protein. *J. Nutr.* **121:** 900–907.
31. Hwang, C. S., and P. E. Kolattukudy. 1993. Molecular cloning and sequencing of thioesterase B cDNA and stimulation of expression of the thioesterase B gene associated with hormonal induction of peroxisome proliferation. *J. Biol. Chem.* **268:** 14278–14284.
32. Cho, H., and J. E. Cronan. 1993. *Escherichia coli* Thioesterase I: molecular cloning and sequencing of the structural gene and identification as a periplasmic enzyme. *J. Biol. Chem.* **268:** 9238–9245.
33. Poulose, A. J., L. Rogers, T. M. Cheesbrough, and P. E. Kolattukudy. 1985. Cloning and sequencing of the cDNA for S-acyl fatty acid synthase thioesterase from the uropygial gland of mallard duck. *J. Biol. Chem.* **260:** 15953–15958.
34. Randhawa, Z. I., and S. Smith. 1987. Complete amino acid sequence of the medium-chain S-acyl fatty acid synthetase thio ester hydrolase from rat mammary gland. *Biochemistry.* **26:** 1365–1373.
35. Poulose, A. J., L. Rogers, and P. E. Kolattukudy. 1981. Primary structure of a chymotryptic peptide containing the "active serine" of the thioesterase domain of fatty acid synthase. *Biochem. Biophys. Res. Commun.* **103:** 377–384.
36. Schweizer, M., K. Takabayashi, T. Laux, K. F. Beck, and R. Schreglmann. 1989. Rat mammary gland fatty acid synthase: localization of the constituent domains and two functional polyadenylation/termination signals in the cDNA. *Nucleic Acids Res.* **17:** 567–586.
37. Jayakumar, A., S. S. Chirala, A. C. Chinault, A. Baldini, L. Abu-Elheiga, and S. J. Wakil. 1994. Isolation and chromosomal mapping of genomic clones encoding the human fatty acid synthase gene. *Genomics.* **23:** 420–424.
38. Fiedorek, F. T., and E. S. Kay. 1994. Mapping of PCR-based markers for mouse chromosome 4 on a backcross penetrant for the misty (m) mutation. *Mamm. Genome.* **5:** 479–485.
39. Shrago, E., T. Spennata, and E. S. Gordon. 1969. Fatty acid synthesis in human adipose tissue. *J. Biol. Chem.* **244:** 2761–2766.
40. Pullinger, C. R., J. D. North, B-B. Teng, V. A. Rifici, A. E. Ronhild de Brito, and J. Scott. 1989. The apolipoprotein B gene is constitutively expressed in HepG2 cells: regulation of secretion by oleic acid, albumin, and insulin, and measurement of the mRNA half-life. *J. Lipid Res.* **30:** 1065–1077.
41. Barnard, E. A. 1969. Ribonucleases. *Annu. Rev. Biochem.* **38:** 677–732.
42. Singer, R. H., and S. Penman. 1973. Messenger RNA in HeLa cells: kinetics of formation and decay. *J. Mol. Biol.* **78:** 321–334.
43. Chen, C. Y. A., T. M. Chen, and A. B. Shyu. 1994. Interplay of two functionally and structurally distinct domains of the c-fos AU-rich element specifies its mRNA-destabilizing function. *Mol. Cell. Biol.* **14:** 416–426.
44. Shaw, G., and R. Kamen. 1986. A conserved AU sequence from the 3′ untranslated region of GM-CSF mRNA mediates selective mRNA degradation. *Cell.* **46:** 659–667.
45. Kimelman, D., and M. W. Kirschner. 1989. An antisense mRNA directs the covalent modification of the transcript encoding fibroblast growth factor in xenopus oocytes. *Cell.* **59:** 687–696.
46. Hildebrandt, M., and W. Nellen. 1992. Differential antisense transcription from the dictyostelium EB4 gene locus: implications on antisense-mediated regulation of mRNA stability. *Cell.* **69:** 197–204.
47. Morris, D. R., T. Kakegawa, R. L. Kaspar, and M. W. White. 1993. Polypyrimidine tracts and their binding proteins: regulatory sites for posttranscriptional modulation of gene expression. *Biochemistry.* **32:** 2931–2937.
48. Zhang, W., B. J. Wagner, K. Ehrenman, A. W. Schaefer, C. T. DeMaria, D. Crater, K. DeHaven, L. Long, and G. Brewer. 1993. Purification, characterization, and cDNA cloning of an AU-rich element RNA-binding protein, AUF1. *Mol. Cell. Biol.* **13:** 7652–7665.
49. Nachaliel, N., D. Jain, and Y. Hod. 1993. A cAMP-regulated RNA-binding protein that interacts with phosphoenolpyruvate carboxykinase (GTP) mRNA. *J. Biol. Chem.* **268:** 24203–24209.
50. Dodson, R. E., and D. J. Shapiro. 1994. An estrogen-inducible protein binds specifically to a sequence in the 3′ untranslated region of estrogen-stabilized vitellogenin mRNA. *Mol. Cell. Biol.* **14:** 3130–3138.
51. Binder, R., S. P. L. Hwang, R. Ratnasabapathy, and D. L. Williams. 1989. Degradation of apolipoprotein II mRNA occurs via endonucleolytic cleavage at 5′-AAU-3′/5′-UAA-3′ elements in single-stranded loop domains of the 3′-noncoding region. *J. Biol. Chem.* **264:** 16910–16918.
52. Schiavi, S. C., J. G. Belasco, and M. E. Greenberg. 1992. Regulation of proto-oncogene mRNA stability. *Biochim. Biophys. Acta.* **1114:** 95–106.
53. Steel, D. M., J. T. Rogers, M. DeBeer, F. C. DeBeer, and A. S. Whitehead. 1993. Biosynthesis of human acute-phase serum amyloid A protein (A-SAA) in vitro: the roles of mRNA accumulation, poly(A) tail shortening and translational efficiency. *Biochem. J.* **291:** 701–707.
54. Shyu, A. B., J. G. Belasco, and M. E. Greenberg. 1991. Two distinct destabilizing elements in the c-fos message trigger deadenylation as a first step in rapid mRNA decay. *Genes & Dev.* **5:** 221–231.